

Porphyrin sensitized solar cells: TiO₂ sensitization with a π -extended porphyrin possessing two anchoring groups†

Chang Yeon Lee, Chunxing She, Nak Cheon Jeong and Joseph T. Hupp*

Received 6th March 2010, Accepted 24th June 2010

DOI: 10.1039/c0cc00257g

A π -extended porphyrin possessing two anchoring groups has been synthesized and successfully applied to dye-sensitized solar cells with a power conversion efficiency of 5.5%, rendering it comparable to the performance of N719-sensitized solar cells under the conditions employed here.

Dye-sensitized solar cells (DSSCs) have attracted much attention as promising alternatives to silicon technology for conversion of solar radiation to electricity.¹ Based on nanostructured metal-oxide semiconductors coated with molecular chromophores, they comprise low-cost materials and can be readily assembled *via* inexpensive, low-tech manufacturing techniques (*e.g.* screen printing, spray pyrolysis, *etc.*). The best DSSCs have achieved energy conversion efficiencies of +11% at 1 sun.² With the aim of pushing device performance significantly higher, the three delicately balanced components of DSSCs—dye, redox shuttle and semiconducting electrode—have been investigated independently.³ In particular, efforts have been made to develop better-performing dyes based on modified ruthenium polypyridyl complexes⁴ and on numerous organic dyes,⁵ including porphyrins.⁶ Among them, porphyrins have received considerable attention due to their remarkably high extinction coefficients compared to ruthenium polypyridyl complexes. Other than a few promising reports by Officer *et al.*,^{6c,d} however, most porphyrin-sensitized solar cells exhibit lower performance than ruthenium polypyridyl complex-sensitized cells despite similar charge transfer dynamics for the two types of systems.⁷ The low performance of porphyrin sensitized solar cells can be partially attributed to a mismatch of the porphyrin absorption spectrum and the solar spectrum, as suggested by recently reported systems using π -extended porphyrins^{6a} and accessory pigment-attached porphyrins⁸ that enhance their absorption in the red region of the solar spectrum. Additionally, we note that binding through four anchoring groups^{6f} (instead of just one) has previously been shown to improve conversion efficiencies.

We herein report the synthesis, characterization and photovoltaic performance of a novel porphyrin dye (**ZnPDCA**†, see Chart 1) with extended π conjugation and two anchoring groups as a sensitizer in DSSCs, and compare the dye to a similar dye (**ZnPcA**†) with only one anchoring group. **ZnPDCA**-sensitized cells show superior performance

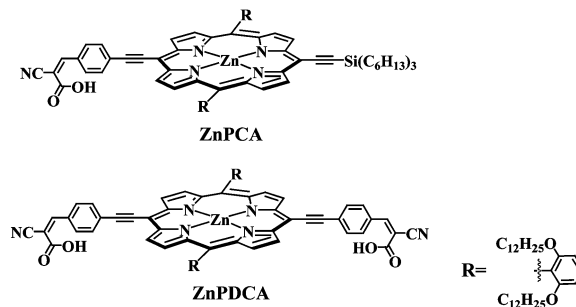


Chart 1 Molecular structures of porphyrin dyes.

(conversion efficiency of 5.5%) to **ZnPcA**-sensitized cells (3.5%) due to better light harvesting and higher efficiency for net charge separation.

ZnPcA and **ZnPDCA** were synthesized by modifying (see ESI†) previously published procedures for related compounds.⁹ Fig. 1 shows the absorption spectra of **ZnPcA** and **ZnPDCA** in methanol and on TiO₂ films. Compounds **ZnPcA** and **ZnPDCA** exhibit typical porphyrin absorption features with strong B bands in the range 400–500 nm and moderate Q bands in the range 600–700 nm. Compared to its parent molecule—an ethynyl bridged porphyrin lacking the acidic anchoring groups (see Fig. S1, ESI†)—the B bands of these dyes are red-shifted and broadened, and Q bands are red-shifted and intensified. These spectral changes indicate effective π -elongation^{6a,10} through the porphyrin ring, ethynyl, and cyanoacrylic acid, with better conjugation for **ZnPDCA**. While redder for **ZnPDCA** than **ZnPcA**, the spectra have similarly narrow bandwidths in solution. For both dyes, absorption bands on TiO₂ films¹¹ are broadened and slightly shifted. However, the Q-band of **ZnPDCA**/TiO₂ shows a larger blue-shift compared with that of **ZnPcA**/TiO₂, suggesting that the environment of **ZnPDCA** on the metal-oxide surface is distinct from that of **ZnPcA**. Notably, the absorbance differences translate into greater total light-harvesting efficiency (LHE) for **ZnPDCA**/TiO₂ than **ZnPcA**/TiO₂.

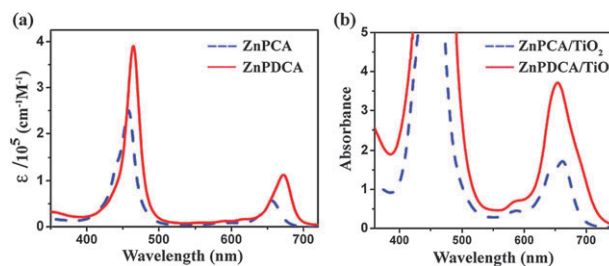


Fig. 1 UV-Vis absorption spectra of **ZnPcA** and **ZnPDCA** (a) in chloroform–ethanol (3 : 1) and (b) on TiO₂ (6 μ m thick nanocrystalline films).

Department of Chemistry, Northwestern University, 2145 Sheridan Road, Evanston, IL 60208, USA. E-mail: j-hupp@northwestern.edu; Fax: +1 847-491-7713; Tel: +1 847-491-3504

† Electronic supplementary information (ESI) available: Details of synthesis, characterization, cyclic voltammetry, DFT molecular orbitals, LHE for **ZnPDCA** and **ZnPcA**, Charge lifetime *versus* photovoltage for **ZnPDCA** and **ZnPcA** sensitized cells, ¹H-NMR spectra and MALDI-TOF. See DOI: 10.1039/c0cc00257g

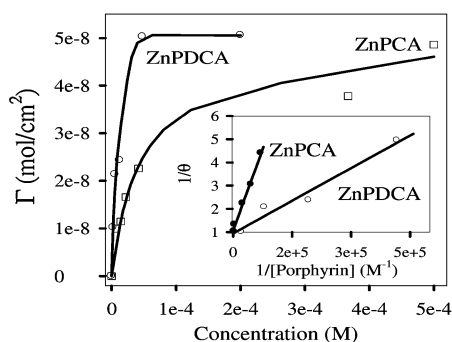


Fig. 2 (a) Surface coverage (Γ , mol cm $^{-2}$) versus solution concentration for **ZnPCA** and **ZnPDCA** adsorbed on TiO $_2$. (b) Double reciprocal plot for **ZnPCA**/TiO $_2$ and **ZnPDCA**/TiO $_2$ expressed as fractional surface coverage, θ .

For 12- μ m thick electrodes in the region 400 to 800 nm, integrated LHEs differ by a factor of 1.23 (Fig. S2, ESI †).

The surface binding abilities of **ZnPCA** and **ZnPDCA** were evaluated by monitoring changes in absorbance of dye/TiO $_2$ films 12 after soaking films for 24 h in CHCl $_3$: EtOH (v : v = 3 : 1) dye solutions of various concentrations. It was assumed that the oscillator strength (but not individual extinction coefficients) over the range 400 to 800 nm equalled those for the dye in solution. 13 Fig. 2 shows Langmuir isotherms 14 for the two dyes. The inset shows double reciprocal plots of the data expressed as fractional surface coverage (θ). Analyses of the double reciprocal plots yielded binding constants of 2.0×10^4 M $^{-1}$ and 1.1×10^5 M $^{-1}$ for **ZnPCA** and **ZnPDCA**, respectively. Speculatively, the five-fold stronger binding of **ZnPDCA** compared to **ZnPCA** might be due to differing binding geometries and/or the fact that **ZnPDCA** has two anchoring groups. Notably, the dyes completely resisted desorption when the photoelectrodes were exposed to aqueous base or to any of the several organic solvents. 15 For photovoltaic measurements, films were soaked for 2 h in 0.5 mM dye solutions. For both dyes, the surface coverage, Γ , was 5×10^{-8} mol cm $^{-2}$ ($\approx 6 \times 10^{-8}$ mol mg $^{-1}$ TiO $_2$). The latter value is somewhat greater (~ 1.3 to $2\times$) than typically reported for porphyrins, 6h,j,16 but it should be noted that for a given dye areal density (mol cm $^{-2}$), coverages expressed in units of mol mg $^{-1}$ will vary with both TiO $_2$ particle size and extent of sintering.

Ground-state oxidation potentials (E_{ox}) of the porphyrin dyes on TiO $_2$ were measured by cyclic voltammetry (CV) using 0.1 M tetrabutylammonium hexafluorophosphate in dichloromethane as the supporting electrolyte. The CVs of **ZnPCA** and **ZnPDCA** indicate that the first oxidation occurs at 1.05 and 1.03 V vs. NHE, respectively (see Fig. S3, ESI †). The excited-state oxidation potentials (E^*_{ox}) of the porphyrin dyes, which can be calculated using the oxidation potential and the E_{0-0} value determined from the intercept of the normalized absorption and emission spectra, namely, $E^*_{ox} = E_{ox} - E_{0-0}$, are -0.92 and -0.82 V, respectively, for **ZnPCA** and **ZnPDCA**. The excited-state potentials are substantially more negative than the conduction-band-edge of TiO $_2$ in contact with the DSSC electrolyte (ca. -0.5 V vs. NHE), 17 indicating favorable energetics for electron injection. In addition, the ground-state oxidation potentials are sufficiently positive of the potential of

I $_3^-$ /I $^-$ (ca. $+0.5$ V vs. NHE) 3 that efficient regeneration with I $^-$ should be feasible.

To gain insight into the electronic structures of **ZnPCA** and **ZnPDCA**, DFT calculations were performed. Geometry optimization was carried out at the B3LYP/6-31G* level. No negative values were observed in the analysis of vibrational frequencies, 6c,d indicating the energy minimum of the geometries. The LUMOs of porphyrin dyes are fully delocalized over the porphyrin ring and entire anchoring groups (see Fig. S4, ESI †). Thus, good electronic coupling between the excited states of the porphyrin dyes and 3d orbitals of TiO $_2$ should be achievable in these systems.

DSSCs were fabricated using **ZnPCA** and **ZnPDCA** as photosensitizers for nanocrystalline TiO $_2$ (~ 20 nm particle diameter) with a thickness of 12 μ m and a scattering layer (4 μ m thick) of 400 nm diameter particles (see ESI †). Fig. 3a shows the photocurrent density–voltage (J – V) curves of the cells. Under AM 1.5 illumination, the **ZnPDCA**-sensitized cell exhibits a short circuit photocurrent density (J_{sc}) of 11.3 mA cm $^{-2}$, an open circuit voltage (V_{oc}) of 680 mV, and fill factor (FF) of 0.70, yielding an overall conversion efficiency (η), derived from the equation $\eta = J_{sc} \times V_{oc} \times FF/\text{input radiation power}$, of 5.5%. On the other hand, the **ZnPCA**-sensitized cell gives a J_{sc} of 7.5 mA cm $^{-2}$, V_{oc} of 660 mV, and FF of 0.69, yielding an η of 3.5%. The power conversion efficiency of **ZnPDCA** with two cyano acrylic acids as anchoring groups is comparable to that for N719 (Fig. 3a) under the conditions employed here, but is superior to that for **ZnPCA** with one cyano acrylic acid.

The incident monochromatic photon-to-current conversion efficiencies (IPCEs) of cells based on **ZnPCA**, **ZnPDCA**, and N719 as sensitizers are shown in Fig. 3b. The IPCE plot for the **ZnPCA**/TiO $_2$ cell is similar to the corresponding absorption spectrum (Fig. 1b). The IPCE spectrum of the **ZnPDCA**/TiO $_2$ cell in the Q-band region is intensified and extended to the near-IR compared to those of **ZnPCA**/TiO $_2$ and N719/TiO $_2$ cells.

The integrated IPCE value for **ZnPDCA** is higher than **ZnPCA** by a factor of ~ 1.6 , consistent with the difference in J_{sc} or the total efficiency (differ by ~ 1.5). The IPCE is the product of the light-harvesting efficiency (η_{lhc}), the net charge injection efficiency (i.e. injection minus geminate recombination with the dye) (η_{inj}), and the electron collection efficiency (η_{col}). From Fig. S2 (ESI †), a factor of 1.23 can be attributed to differences in the integrated η_{lhc} due to the higher extinction of **ZnPDCA**. As to η_{col} , measurements of open-circuit

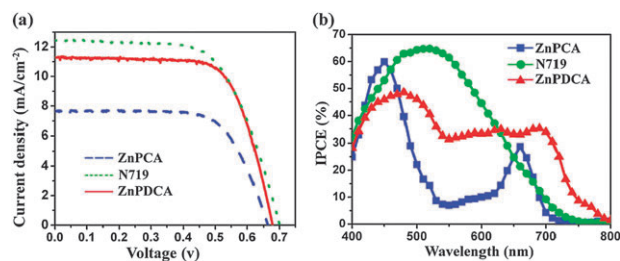


Fig. 3 (a) J – V curves of **ZnPCA**, **ZnPDCA** and N719 sensitized solar cells. (b) IPCE values of **ZnPCA**, **ZnPDCA** and N719 sensitized solar cells.

photovoltage decay (OCPD)¹⁸ were performed for evaluating comparative charge-collection dynamics. OCPD measures the dynamics of interception of photogenerated electrons by the redox electrolyte, thus indirectly reflecting the charge collection dynamics which competes with interception. **ZnPDCA** and **ZnPCA** based cells yielded nearly identical decay curves, indicating nearly identical charge collection dynamics and implying nearly identical η_{col} values (see Fig. S5, ESI†). By default, we conclude that differences in net injection efficiency most likely account for the remaining difference in IPCE behavior for **ZnPDCA** versus **ZnPCA** based cells. Thus, η_{inj} for **ZnPDCA** appears to be $\sim 1.3\times$ higher than that for **ZnPCA**.

Higher injection efficiencies for ruthenium complexes with increased number of carboxyl groups have been suggested previously.¹⁹ Aranyos *et al.*^{19a} observed that the efficiency for a ruthenium complex with monocarboxylate was inferior to that of a complex with dicarboxylate and concluded that the differences in DSSC performance are most likely due to differences in η_{inj} . Hara *et al.*^{19b} reported that two anchoring groups are necessary for large molecules to adhere to TiO₂ surfaces with an anchoring geometry favorable for injecting electrons efficiently. Moreover, it has been reported that planar dye binding geometries can lead to higher DSSC efficiencies.^{6b,j,k} Rochford *et al.*^{6j} reported greater efficiency for a rigid planar meta-substituted porphyrin with four anchoring groups and Campbell *et al.*^{6b} observed a five-fold increase in porphyrin-derived J_{sc} for a dye in flat binding mode compared to one featuring edgewise binding. We speculate that binding geometries may differ for **ZnPCA** and **ZnPDCA**.

In summary, the π -extended porphyrin, **ZnPDCA**, possessing two anchoring groups has been synthesized and found to yield an overall energy conversion efficiency of 5.5%. **ZnPDCA**-sensitized cells showed a 60% increase in cell performance compared with **ZnPCA**-sensitized cells due to: (a) gains in light harvesting efficiency (improved far-red absorption) and (b) (apparently) improved net charge injection efficiency. This work should contribute to the development of anchoring moieties capable of enhancing the performance of porphyrin based DSSCs. Detailed kinetic studies of the **ZnPDCA** and **ZnPCA** based cells will be carried out to determine absolute injection efficiencies for these two dyes.

We thank Rebecca A. Jensen and Chaiya Prasittichai for helpful discussions. We gratefully acknowledge support for NCJ via a National Research Foundation of Korea Grant (NRF-2009-352-D00055). We also thank the U. S. Dept. of Energy's Office of Science (grant No. DE-FG87ER13808) for support of our work.

Notes and references

- (a) B. O'Regan and M. Grätzel, *Nature*, 1991, **353**, 737; (b) M. Grätzel, *Nature*, 2001, **414**, 338; (c) M. Grätzel, *J. Photochem. Photobiol., C*, 2003, **4**, 145; (d) A. Hagfeldt and M. Grätzel, *Acc. Chem. Res.*, 2000, **33**, 269; (e) M. Grätzel, *Inorg. Chem.*, 2005, **44**, 6841.
- M. K. Nazeeruddin, F. DeAngelis, S. Fantacci, A. Selloni, G. Viscardi, P. Liska, S. Ito, B. Takeru and M. Grätzel, *J. Am. Chem. Soc.*, 2005, **127**, 16835.

- (a) T. W. Hamann, R. A. Jensen, A. B. F. Martinson, H. Van Ryswyk and J. T. Hupp, *Energy Environ. Sci.*, 2008, **1**, 66; (b) A. B. F. Martinson, T. W. Hamann, M. J. Pellin and J. T. Hupp, *Chem.–Eur. J.*, 2008, **14**, 4458.
- N. Robertson, *Angew. Chem., Int. Ed.*, 2006, **45**, 2338.
- (a) A. Mishra, M. K. R. Fischer and P. Bäuerle, *Angew. Chem., Int. Ed.*, 2009, **48**, 2474; (b) S. Ito, S. M. Zakeeruddin, R. Humphry-Baker, P. Liska, R. Charvet, P. Comte, M. K. Nazeeruddin, P. Péchy, M. Takata, H. Miura, S. Uchida and M. Grätzel, *Adv. Mater.*, 2006, **18**, 1202; (c) S. Hwang, J. H. Lee, C. Park, H. Lee, C. Kim, C. Park, M.-H. Lee, W. Lee, J. Park, K. Kim, N.-G. Park and C. Kim, *Chem. Commun.*, 2007, 4887; (d) T. Horiuchi, H. Miura, K. Sumioka and S. Uchida, *J. Am. Chem. Soc.*, 2004, **126**, 12218.
- (a) H. Imahori, T. Umeyama and S. Ito, *Acc. Chem. Res.*, 2009, **42**, 1809; (b) W. M. Campbell, A. K. Burrell, D. L. Officer and K. W. Jolley, *Coord. Chem. Rev.*, 2004, **248**, 1363; (c) Q. Wang, W. M. Campbell, E. E. Bonfantani, K. W. Jolley, D. L. Officer, P. J. Walsh, K. Gordon, R. Humphry-Baker, M. K. Nazeeruddin and M. Grätzel, *J. Phys. Chem. B*, 2005, **109**, 15397; (d) W. M. Campbell, K. W. Jolley, P. Wagner, K. Wagner, P. J. Walsh, K. C. Gordon, S.-M. Lukas, M. K. Nazeeruddin, Q. Wang, M. Grätzel and D. L. Officer, *J. Phys. Chem. C*, 2007, **111**, 11760; (e) M. Tanaka, S. Hayashi, S. Eu, T. Umeyama, Y. Matano and H. Imahori, *Chem. Commun.*, 2007, 2069; (f) C.-W. Lee, H.-M. Lan, Y.-L. Huang, Y.-R. Liang, W.-N. Yen, Y.-C. Liu, Y.-S. Lin, E. W.-G. Diau and C.-Y. Yeh, *Chem.–Eur. J.*, 2009, **15**, 1403; (g) J. K. Park, H. R. Lee, J. P. Chen, H. Shinokubo, A. Osuka and D. Kim, *J. Phys. Chem. C*, 2008, **112**, 16691; (h) C. Y. Lin, C. F. Lo, L. Luo, H. P. Lu, C. S. Hung and E. W. G. Diau, *J. Phys. Chem. C*, 2009, **113**, 755; (i) J. K. Park, J. Chen, H. R. Lee, S. W. Park, H. Shinokubo, A. Osuka and D. Kim, *J. Phys. Chem. C*, 2009, **113**, 21956; (j) J. Rochford, D. Chu, A. Hagfeldt and E. Galoppini, *J. Am. Chem. Soc.*, 2007, **129**, 4655; (k) N. R. Tacconi, W. Chanmanee, K. Rajeshwar, J. Rochford and E. Galoppini, *J. Phys. Chem. C*, 2009, **113**, 2996.
- Y. Tachibana, S. A. Haque, I. P. Mercer, J. R. Durrant and D. R. Klug, *J. Phys. Chem. B*, 2000, **104**, 1198.
- C. Y. Lee and J. T. Hupp, *Langmuir*, 2010, **26**, 3760.
- C.-H. Lee and J. D. Lindsey, *Tetrahedron*, 1994, **50**, 11427.
- V. S.-Y. Lin, S. G. DiMagno and M. J. Therien, *Science*, 1994, **264**, 1105.
- In order to display the Q-bands, we show absorption spectra for 6 μm thick dye/TiO₂ films. In the fabricated DSSCs, TiO₂ films are 12 μm thick; see spectra in Fig. S2 (ESI†).
- Film surface areas and porosity (66%) were determined via BET analysis of N₂ adsorption by a thick sample of nanoparticulate TiO₂.
- Calculations using only the integrated Q bands (570 nm to 800 nm) yielded identical results.
- T. J. Meyer, G. J. Meyer, B. W. Pfennig, J. R. Schoonover, C. J. Timpson, J. F. Wall, C. Kobusch, X. Chen, B. M. Peek, C. G. Wall, W. Ou, B. W. Erickson and C. A. Bignozzi, *Inorg. Chem.*, 1994, **33**, 3952.
- MeOH, THF, CH₃CN, DMF, and 0.1 M aq. NaOH were examined.
- S. Cherian and C. C. Wamser, *J. Phys. Chem. B*, 2000, **104**, 3624.
- P. V. Kamat, M. Haria and S. Hotchandani, *J. Phys. Chem. B*, 2004, **108**, 5166.
- See, for example: (a) A. Zaban, M. Greenshtein and J. Bisquert, *ChemPhysChem*, 2003, **4**, 859; (b) A. B. Walker, L. M. Peter, K. Lobato and P. J. Cameron, *J. Phys. Chem. B*, 2006, **110**, 25504; (c) C. Prasittichai and J. T. Hupp, *J. Phys. Chem. Lett.*, 2010, **1**, 1611.
- (a) V. Aranyos, H. Grennberg, S. Tingry, S.-E. Lindquist and A. Hagfeldt, *Sol. Energy Mater. Sol. Cells*, 2000, **64**, 97; (b) K. Hara, H. Sugihara, Y. Tachibana, A. Islam, M. Yanagiba, K. Sayama and H. Arakawa, *Langmuir*, 2001, **17**, 5992.